Characterization of Tin Substituted Fe2TiO5 Based Materials

Dr. Sandesh Suryakant Gurav*

Principal, K.E.S. Anandibai Pradhan Science College, Nagothane, Tahsheel-Roha, District-Raigad, University of Mumbai

Abstract – In order to study the characterization of the tin substituted Fe2TiO5 based materials the samples are prepared by standard ceramic technique. The single-phase formation of the pseudobrookite is confirmed by XRD technique.

It is interesting to note that substitution of Ti 4+ by Sn4+ is responsible to increase the unit cell volume and X-Ray or theoretical density. On the other hand, the use of anatase in the reaction causes the decrease in practical density and the increase in the porosity, Debye particle size and the inhomogeneity.

Key words: Substitution, Pseudobrookite.

----------X----------

1. INTRODUCTION:

Iron titanate is a pseudobrookite which exhibits many interesting properties such as spin glass behaviour, thermal microcracking, high resistivity, etc. A cluster approach may be used for a description of spin glass behaviour of the pseudobrookites [1]. D. A. Kharmov, et.al [1] have studied the spin glass transition in the $Fe_2 Ti_{1-x} Sn_x O_5$ pseudobrookite and found that Sn^{4+} ions appear to occupy only M1/ 4c octahedral sites and spin glass transition temperature T_g depends on tin concentration monotonically. According to the XRD analysis and Sn-Mossbauer Spectral (MS) data the maximum solubility of Sn^{4+} ions in the pseudobrookite structure at 1250^{o}C is x = 0.22 [1], where the unit cell volume increases linearly with the increasing tin concentration.

The XRD analysis of the limit of solid solution $Fe_2 Ti_{1-x} Sn_x O_5$ ($0<x<0.25$) has been conducted by S. S. Meshalkin et al. [2] and has obtained x = 0.18 as the limit. A spin relaxation model has been used by G. M. Irwin et al. [3] However, the data of electrical transport and dielectric properties of the tin containing pseudobrookite is scarce [4].

SnO_2 (sintered ceramics and also compressed powder under very high pressure) exhibits an astonishingly high value of dielectric constant of the order of 10^5 [5] It is observed that small amount of SnO_2 doping enhances the rutilation of anatase and effectively prohibits the grain growth in these powders [6]. The incorporation of about 17% of Sn completely transforms anatase to the rutile form at a calcination temperature as low as 500^{o}C [7]. The optical analysis shows that the band gap and Fermi level of the$Ti_{1-x} Sn_x O_2$ solid solutions increases with increasing x and these solid solutions are expected to be of better photocatalytic properties [7].However, the grain boundary barrier or energy barrier is ineffective. The solubility of Ti^{4+} ions in SnO_2 is up to 25 mole %.

SnO_2 has been supported on TiO_2 , Al_2O_3 , MgO and SiO_2 [8-9] and the resulting interactions between the components in the prepared samples and after reduction in flowing hydrogen by slowly raising the temperature from ambient to the reduction temperature are characterized by Mossbauer Spectral (MS) data. It is found that on titania a smaller Quadrupole Splitting (QS) is observed, which might be explained assuming that Sn^{4+} is inside the structure of the titania. This is in agreement with the findings reported by Bartholomew and Boudart [10], who have reported that the Quadrupole Splitting (QS) for an atom in a crystal is lower than on the surface. The reduction of the species is easier if it is present on the surface than within the structure of support. The results obtained for tin on titania agree with this fact. Therefore, tin is present on the surface as well as within the structure of titania [9].

Ceramic bodies have been prepared from the ferric stannates and their dielectric properties have been measured [11]. They are found to be semiconductor. The substitution of Sn^{4+} ion for the Ti^{4+} ion may also be expected to improve the stability of titanate bodies with regard to changes in the state of oxidation during normal firing treatment, since SnO_2 is more stable in this respect than TiO_2 [12]. The study of Reitveld structure refinement of XRD of tin doped α-Fe_2O_3 has been reported to contain tin in both interstitial and

substitutional sites of the corundum-related α-Fe_2O_3 structure [13].

2. RESULTS AND DISCUSSION:

2.1 Structural Properties:

The structural properties of the samples namely Fe_2TiO_5 using rutile TiO_2 [FTR], Fe_2TiO_5 using anatase TiO_2 [FTA], Fe_2 $Ti_{0.75}$ $Sn_{0.25}$ O_5 using rutile TiO_2 [FTSR] and Fe_2 $Ti_{0.75}$ $Sn_{0.25}$ O_5 using anatase TiO_2 [FTSA] all synthesized at 1250°C are reported here. The corresponding XRD data is reported in

Figures 1-4 and Tables1-4 respectively. The data is indexed in a single phase orthorhombic structure having the space group Bbmm of the pseudobrookite.

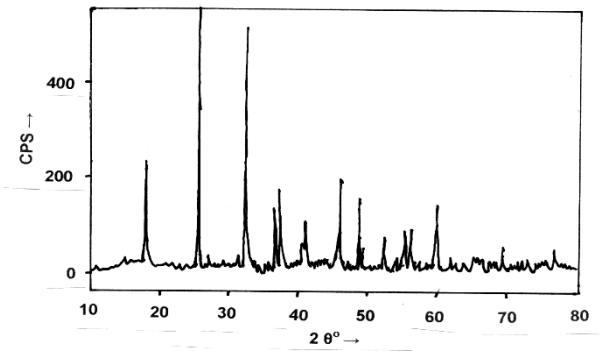

Figure -1: The X-Ray diffraction pattern for sample [FTR].

Table - 1: X-Ray diffraction data for Fe_2TiO_5 (using rutile TiO_2).i. e. [FTR]

Space group: Bbmm, Lattice parameters;a=9.7780 Å, b=9.9608 Å, c=3.7262 Å.

d_{obs} Å	I/Io %	hkl	d_{cal} Å	Debye Particle size Å
4.8888	41.2	200	4.8890	600
3.4819	100	101	3.4810	610
3.2883	7.6	111	3.2860	620
2.8502	6.4	121	2.8530	
2.747	86.9	230	2.7460	626
2.4866	1.6	040	2.4900	
2.4515	17.1	301	2.4530	502
2.4030	22.7	131	2.4029	502
2.219	10	240	2.2189	
2.1942	16	420	2.1944	318
1.9690	23.2	430	1.9685	431
1.8635	29.6	002	1.8631	522
1.8445	5.3	250	1.8448	
1.7468	6.5	341	1.7476	
1.6618	14	060	1.6601	
1.6365	18	521	1.6355	
1.6075	4.5	610	1.6082	
1.5674	1.4	260	1.5719	
1.5448	6.5	450	1.5442	
1.5365	21.8	531	1.5353	

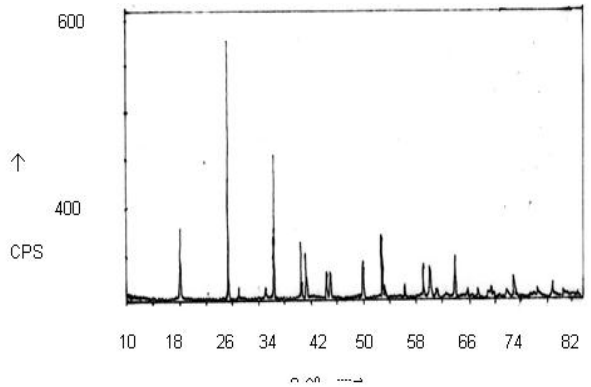

Figure- 2: The X-Ray diffraction pattern for sample [FTA].

Table-2:X-Ray Diffraction data for Fe_2TiO_5 (using anatase TiO_2)**. .i.e. [FTA].**

Space group: Bbmm, Lattice parameters; a =9.795 Å, b=9.992 Å, c=3.732 Å.

dobs Å	I/Io %	hkl	dcal Å	Debye Particle size Å
4.996	8	020	4.996	
4.898	26	200	4.898	619
3.488	100	101	3.487	626
3..293	6	111	3.293	
2..859	5	121	2.861	
2.753	44	230	2.756	636
2.456	21	301	2.457	644
2.408	16	131	2.408	645
2.385	3	311	2.387	
2.224	12	240	2.225	
2.198	12	420	2.199	
1.973	14	430	1.973	
1.867	26	002	1.866	
1.848	8	250	1.851	
1.751	6	440	1.749	
1.663	18	060	1.665	
1.639	13	521	1.639	
1.635	7	600	1.633	
1.611	7	610	1.611	
1.608	5	132	1.606	

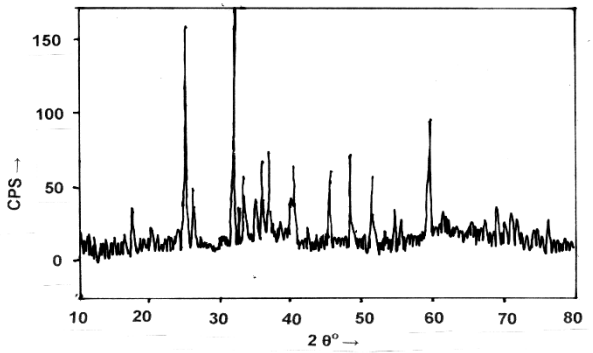

Figure - 3: The X-Ray diffraction pattern for sample [FTSR].

Table -3: X-ray diffraction data for $Fe_2Ti_{0.75}Sn_{0.25}O_5$(using rutile TiO_2).i.e. [FTSR]

Space group: Bbmm , Lattice Parameters:a=10.0655 Å, b=10.0821Å, c=3.7946 Å

d_{obs} Å	I/Io %	hkl	d_{cal} Å	Debye Particle size Å
e5.0327	20.02	200	5.0327	500
3.5506	100	101	3.5506	406
2.7949	105	230	2.7948	495
2.4885	38.5	040	2.5205	500
2.4364	43.47	311	2.4388	418
2.2273	24	240	2.2536	
1.9944	36.3	331	2.0128	397
1.8820	45.36	002	1.8973	434
1.6526	14.28	060	1.6803	
1.5531	47.56	232	1.5697	
1.4308	8.6	242	1.4514	
1.3633	12.3	432	1.3811	
1.3247	7.5	171	1.3346	
1.2473	10.4	062	1.2579	

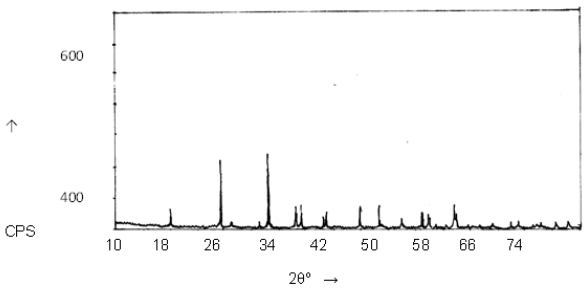

Figure - 4: The X-Ray diffraction pattern for sample [FTSA].

Table -4:X-Ray diffraction data for $Fe_2Ti_{0.75}Sn_{0.25}O_5$(using anatase TiO_2)i.e.[FTSA]

Space group: Bbmm, Lattice parameters; a =9.856 Å, b=10.016 Å, c=3.747 Å.

dobs Å	I/Io %	hkl	dcal Å	Debye Particle size Å
4.928	32	200	4.928	638
3.502	100	101	3.502	635
3.307	15	111	3.306	
2.873	10	121	2.870	
2.764	123	230	1.765	656
2.467	38	301	2.470	669
2.417	43	131	2.416	665
2.233	20	240	2.232	
2.207	34	420	2.210	
1.980	41	331	1.983	
1.872	38	002	1.874	
1.855	10	250	1.856	
1.756	20	440	1.756	
1.669	30	060	1.669	
1.645	24	521	1.648	
1.640	23	600	1.642	
1.617	12	610	1.621	
1.550	38	232	1.551	
1.544	35	531	1.546	
1.471	6	630	1.474	

Hence it is concluded that all the samples [FTR], [FTA], [FTSR] and [FTSA] are pseudobrokites. The values of unit cell volume V, XRD density, practical density, Debye particle size, porosity and inhomogeneity are included in the Table - 5.

Table - 5: Data showing the Unit-cell Volume (V), XRD and Practical Density, Debye particle size, Porosity and Inhomogeneity

Sample	V $(Å)^3$	Density from XRD g/cc	Practical Density g/cc	Debye particle size Å	Porosity	Inhomogeneity
FTR	362.9	4.384	3.999	540	0.09	-0.0020
FTA	365.3	4.356	3.741	634	0.14	-0.0038
FTSR	385.1	4.437	4.289	450	0.03	-0.0025
FTSA	369.9	4.604	3.534	653	0.23	-0.0030

It is interesting to note that substitution of Ti^{4+} by Sn^{4+} is responsible to increase the unit cell volume and X-Ray or theoretical density. This may be attributed to the larger ionic radius and larger atomic mass of Sn^{4+} [14].

On the other hand, the comparison of [FTR] with [FTA] shows that the use of anatase in the reaction causes the decrease in practical density and the increase in the porosity, Debye particle size and the inhomogeneity. This may be attributed to the vertex –sharing network of anatase which is opposite to the edge –sharing network of the pseudobrookite [18].

However, the comparison of [FTR] with [FTSR] and [FTA] with [FTSA] shows that tin has exactly opposite effect on the anatase as the practical density, porosity, inhomogeneity and the Debye particle size are concern. The tendency of tin to increase the practical density or to decrease the porosity and the Debye particle size comes from its abilities to

(i) increase the speed of rutilation and to inhibit the grain growth [6],

(ii) to occupy both interstitial and substitutional sites[13] and

(iii) to be present both on the surface and within the structure [9].

The effect of tin on the porosity and the Debye particle size is however less dominant.

It is thought worthwhile to compare these observations with the cation distributions of these four samples reported in Table - 6 obtain from new empirical model [19] . It is interesting to note that Sn^{4+} occupies only M1 sites. This agrees well with the earlier work [1, 2]. Moreover, the relative percentage intensities of (230) planes which passes through the M1 sites (Figure - 5) increase from 87 in [FTR] to 105 in [FTSR] and 44 in [FTA] to 123 in [FTSA] (Tables 1-

4 and Figures 1-4) implying the occupancy of M1 sites by Sn^{4+}.

Secondly Sn^{4+} displaces Fe^{3+} to M2 sites. Knowing the preference of Fe^{3+} for lower tetrahedral symmetry [18], the symmetry of the M2 site is lowered by Sn^{4+}. Also, the octahedral symmetry that Sn^{4+} prefers raises the symmetry of the M1 site. Overall Sn^{4+} causes net increase in the asymmetry of the pseudobrookite and therefore the increase in volume (Table - 6).

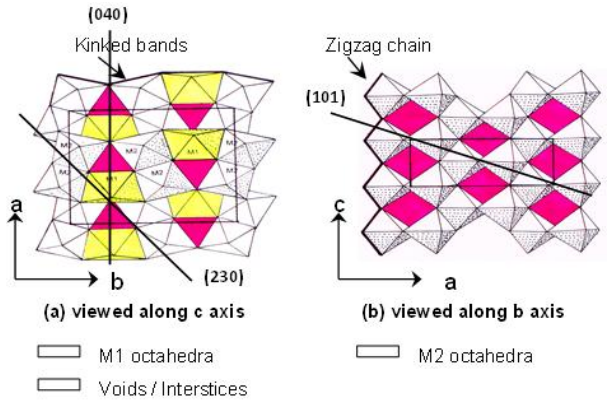

Figure -5: The Pseudobrookite Structure. [17]

Table - 6: Cation Distribution of the samples obtained from new Empirical Model [19]

Sample	Cation distribution	c/ab per Å	q_1/q_2	Order Parameter λ'	Unit cell volume V (Å)³	Relative intensity Of (230) plane	Relative intensity Of (101) plane
[FTR]	$[Fe_{0.78}\ Ti_{0.22}]_{M1}\ [Fe_{1.22}\ Ti_{0.78}]_{M2}\ O_5$	0.03826	0.92	0.310	362.9	86.9	100
[FTA]	$[Fe_{0.6}\ Ti_{0.4}]_{M1}\ [Fe_{1.4}\ Ti_{0.6}]_{M2}\ O_5$	0.03813	0.96	0.040	365.3	44	100
[FTSR]	$[Fe_0\ Sn_{0.25}\ Ti_{0.75}]_{M1}\ [Fe_2\ Ti_0]_{M2}\ O_5$	0.03739	1.37	1.000	385.1	105	100
[FTSA]	$[Fe_{0.37}\ Sn_{0.25}\ Ti_{0.38}]_{M1}\ [Fe_{1.63}\ Ti_{0.37}]_{M2}\ O_5$	0.03796	1.06	0.068	369.9	123	100

Also, more Fe^{3+} shifts to the M2 site when anatase is used in place of rutile. Thus, [FTA] is more asymmetric than [FTR]. This is likely to decrease the practical density, increase the porosity, the Debye particle size and the inhomogeneity.

This trend reverses when one compares the cation distribution of [FTSR] with that of [FTSA] and [FTSR] is now more asymmetric. This is because Sn^{4+} prefers the M1 site [6, 9,13] and attracts rutile Ti^{4+} to the M1 site as both prefer the edge sharing. These effects are summarized by defining the order parameter **λ'** [20] which shows that the order parameter **λ'** is decreased by use of anatase and increased by substitution of Sn^{4+}.

2.2 Cation Distribution and IR-Spectra:

The IR spectra of the samples recorded on the 'PERKIN-ELMER' 683 Spectro Photometer at room temperature are as shown in the Figure -6 and the possible octahedral assignment [4] of two major bands of frequencies ν1 and ν2 corresponding to the octahedral sites M1 and M2 [4] respectively is reproduced in the Table-7.

It is interesting to note that substitution of Ti^{4+} by Sn^{4+} shifts ν1 and ν2 to the high frequency side. On the other hand the use of anatase causes ν1 to shift to lower frequency side and ν2 to shift to higher frequency side. Moreover, the sharpness and the intensity difference increase due to the anatase.

It is observed that both the use of anatase and the substitution of Sn^{4+} decreases the frequency difference (ν1- ν2) between these bands. The shift of ν1 to the high frequency side appears to be due to the larger charge of Sn^{4+} on M1 site. On the other hand, the high frequency shift of ν2 causes from the increase in Fe^{3+} content, having lower symmetry on M2 site. (Figure -6 and Tables- 6 and 7).

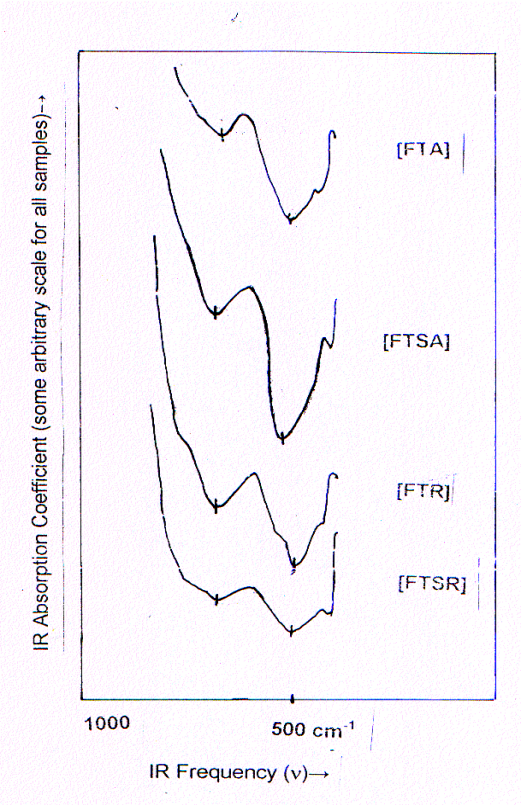

Figure- 6: The IR-Spectra for the samples.

Table -7: Assignment of two major bands of frequencies ν1and ν2 corresponding to the octahedral sites M1 and M2 respectively for the pseudobrookites.

Bands	Frequency (cm^{-1})				Possible octahedral assignment
Sample →	[FTA]	[FTR]	[FTSA]	[FTSR]	
ν1	668	690	682	688	M1
ν2	507	490	534	503	M2
ν1-ν2	161	200	148	185	

3. CONCLUSIONS:

It is interesting to note that substitution of Ti^{4+} by Sn^{4+} is responsible to increase the unit cell volume and X-Ray or theoretical density. On the other hand, the use of anatase in the reaction causes the decrease in practical density and the increase in the porosity, Debye particle size and the inhomogeneity. This may be attributed to the vertex –sharing network of anatase which is opposite to the edge –sharing network of the pseudobrookite.

However, tin has exactly opposite effect on the anatase as the practical density, porosity, inhomogeneity and the Debye particle size are concern.

REFERENCES:

1. D. A. Khramov, M. A. Glazkova, S. S. Meshalkin (1995). J. Magn.Mag. Materials, **150**, pp. 101.

2. S. S. Meshalkin, M. A. Glazkova, D. A. Kharmov, V. S. Urusov (1994). Mater. Sci. Forum, **166-169**, pp. 717.

3. G. M. Irwin, E. R. Sanford (1991). Physical Review B, **44**, 9, pp. 4423-4430.

4. S. V. Salvi, A. H. Karande, M. A. Madare, S. S. Gurav (2005). J. Ferro. and Inte. Ferro., Netherland, **323**, pp. 97.

5. L. V. Deshpande, V. G. Bhide (1960). Lett. Alla Redazione, pp. 816.

6. X. Z. Ding, Z. A. Qi, Y. Z. He (1994). J. Nano Stru. Mater., **4**, 6, pp. 663.

7. S. Mahanty, S. Roy, Suchitra Sen (2004). J. Crys. Growth, **261**, pp. 77.

8. V. Ravi, S. K. Date (2001). Bulle. Mater. Sci., **24**, 5, pp. 483.

9. Noel Nava, Thomas Viveros (1999). Hyperfine Inter. **122**, pp. 147.

10. C. H. Bartholomew, M. Budart (1973). J. Catalysis, **29**, pp. 278.

11. William W. Coffeen (1953). J. Amer. Cer. Soc., **36**, 7, pp. 207.

12. Frank J. Berry, O. Helgason (2000). Hyper. Inter., **126**, pp. 269.

13. F. J. Berry, C. Greaves, J. McManus, M. Mortimer, G. Oates (1997). J. Sol. Stat. Chem.**130**, pp. 272.

14. Linus Pauling, Nature of Chemical Bonds, 3rd Edn. Cornell Univ. Press, Ithac., New York.

15. R. S. Singh, T. H. Ansari, R. A. Singh, B. M. Wanklyn, B. E. Watt (1995). Sol. Stat. Comm., **94**, 12, pp. 103.

16. H. J. Siebeneck, O. P. H. Hasselmann, C. J. Cleveland, R. C. Bradt (1976). J. Am. Ceram. Soc. May-June, pp. 241.

17. T. Birchall, N. N. Greenwood and A. F. Reid (1969). J. Chem. Soc. (**A**) p. 2388.

18. P. T. Supe and K. R. Rao (1974). Current Science, **43**, pp. 377.

19. S. S. Gurav, S. V. Salvi, S. Y. Shingare and A. H. Karande (2014). Global Journal of Science Frontier Research: A physics and space science, Vol. **14,** Issue-4, Version-1.0, p. 13-18.

20. S. S. Gurav (2007). Ph. D. Thesis, University of Mumbai.

Corresponding Author

Dr. Sandesh Suryakant Gurav*

Principal, K.E.S. Anandibai Pradhan Science College, Nagothane, Tahsheel-Roha, District-Raigad, University of Mumbai